ACS APPLIED MATERIALS & INTERFACES

Research Article

www.acsami.org

Role of Chirality and Macroring in Imprinted Polymers with Enantiodiscriminative Power

Jozsef Kupai,[‡] Eszter Rojik,[‡] Peter Huszthy,[‡] and Gyorgy Szekely*[,†]

[‡]Department of Organic Chemistry and Technology, Budapest University of Technology and Economics, Szent Gellért tér 4., Budapest H-1111, Hungary

[†]School of Chemical Engineering and Analytical Science, The University of Manchester, The Mill, Sackville Street, Manchester M13 9PL, United Kingdom

Supporting Information

ABSTRACT: Enantioselective discrimination of chiral amines is of great importance as their biological properties often differ. Therefore, here we report the development of synthetic receptors for their enantioselective recognition and pH-sensitive drug release. This paper reports the preparation of three pyridine and two benzene derivatives containing an allyloxy group [(*S*,*S*)-**5**, **6**–**9**] as well as their evaluation as functional monomer anchors for chiral imprinting of amines. The enantiomeric enriching ability and controlled release of the imprinted polymers (IPs) were evaluated using racemic mixture of 1-(1-naphthyl)ethylamine hydrogen perchlorate (**1**). The effect of the enantiomeric purity of the template on the enantioseparation performance was investigated. Racemic template in combination with enantiomerically pure macrocyclic anchors and vice versa yields IPs with excellent enantiomeric recognition. In vitro drug delivery, enantiomeric enrichment and pH-sensitive release were investigated through kinetic models.

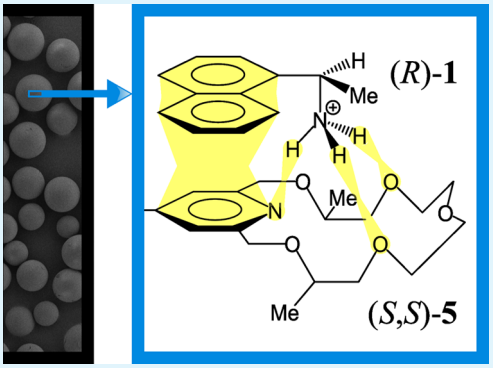

KEYWORDS: *molecularly imprinted polymer, drug delivery, crown compounds, chirality, enantioselectivity*

INTRODUCTION

Chirality is a fundamental property of nature and the development of synthetic receptors with chiral recognition is still a major scientific challenge.[1] In this context, imprinting (Figure 1) is a well-known approach for fabricating materials with enantioselective properties, and it has found various potential applications ranging from catalysis to separation science since the pioneering work of Wulff,[2] Mosbach,[3] and Hosoya.[4,5]

Enantioselective discrimination of chiral molecules is of great importance as their biological properties often differ.[6,7] Chiral amines serve as neurotransmitters in biological systems or being formed during the degradation of amino acids. Therefore, the development of synthetic receptors for their enantioselective recognition is important. Here we report the development of chirally imprinted receptors toward protonated primary aralkylamines and evaluate their potential in pH-sensitive drug delivery and purification of chiral drugs.

Imprinted polymers were fabricated in the presence of 1-(1-naphthyl)ethylamine hydrogen perchlorate (**1**) as template (Figure 2A) and macrocycles (Figure 2B) as functional monomer anchors. Optically active macrocycles containing a pyridine subunit have recently become attractive hosts due to their ability for chiral discrimination toward organic ammonium salt and amino acid derivatives.[8,9]

According to the "three-point rule" enantiomeric recognition requires a minimum of three simultaneous interactions with at least one of these interactions being stereochemically dependent.[10] The interaction of protonated primary aralkylamine enantiomers with pyridino-18-crown-6 ether is 2-fold (Figure 3). The fundamental host–guest interaction is tripod hydrogen bonding involving the nitrogen atom of pyridine and two alternate oxygen atoms of the macroring and three protons of the ammonium cation.[11] Furthermore, the pyridine subunit also has $\pi-\pi$ interactions with the aromatic groups of the ammonium guests.[6] The above-mentioned two attractive interactions involving the pyridine ring result in rather rigid conformations of the diastereomeric complexes of the macrocycles with guest enantiomers.[12] The margin of steric repulsion caused by the different spatial arrangements in the two diastereomeric complexes becomes large and therefore an increase in the degree of enantiomeric recognition is expected in the presence of a pyridine subunit in the macrocycle. The third point of the "three-point rule" is the above-mentioned steric repulsion between the guest and the host molecules. IPs featuring enantiodiscriminative power can be prepared in three different ways: (i) enantiopure functional monomer with enantiopure template; (ii) enantiopure functional monomer with racemate template; and (iii) achiral functional monomer with enantiopure template. Case (ii) involves enantiodiscrimination in the prepolymerization mixture

Received: January 26, 2015
Accepted: April 17, 2015
Published: April 17, 2015

DOI: 10.1021/acsami.5b00755
ACS Appl. Mater. Interfaces 2015, 7, 9516–9525

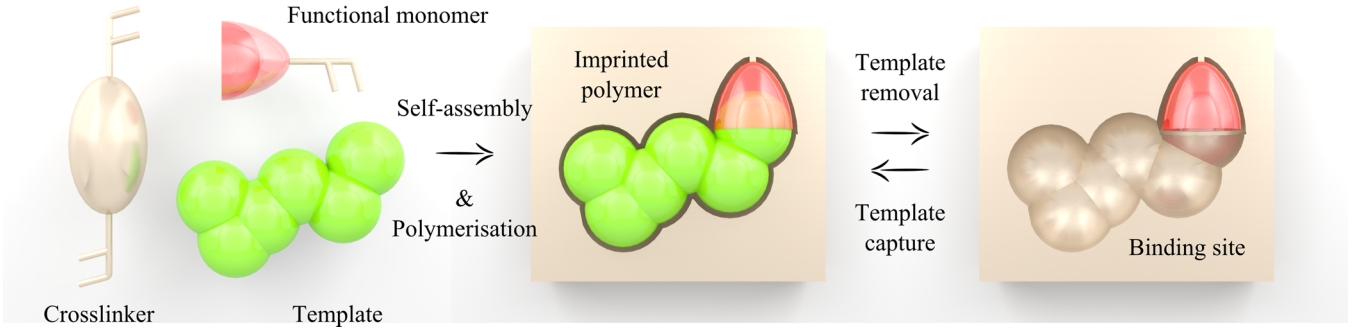

Figure 1. Concept of molecular imprinting. After the self-assembly of the functional monomer, the template, and the cross-linker polymerization yields the scavenger. The template is removed from the polymer leaving a complementary cavity behind. The scavenger can selectively recognize the template in a complex mixture.

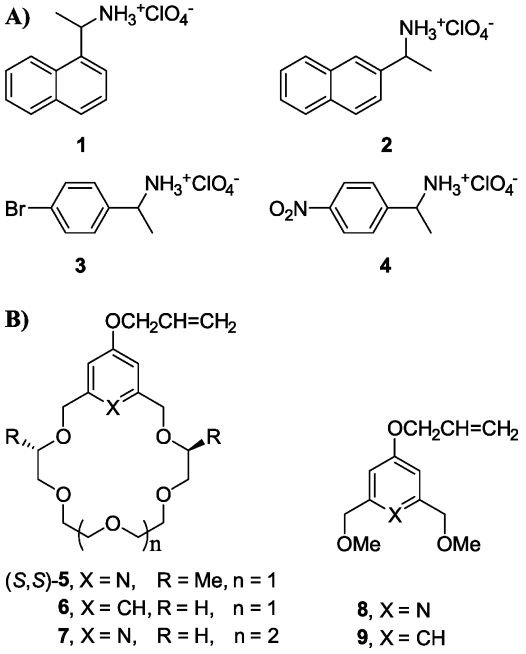

Figure 2. A) Structures of the hydrogen perchlorate salts of aralkylamine analytes: 1-(1-naphthyl)ethylamine (**1**) was used as template, while 1-(2-naphthyl)ethylamine (**2**), 1-(4-bromophenyl)ethylamine (**3**), and 1-(4-nitrophenyl)ethylamine (**4**) were used to probe the selectivity of the polymers. B) Structures of the macrocyclic functional monomers [(*S*,*S*)-**5**−**7**] and their precyclization analogues (**8**−**9**).

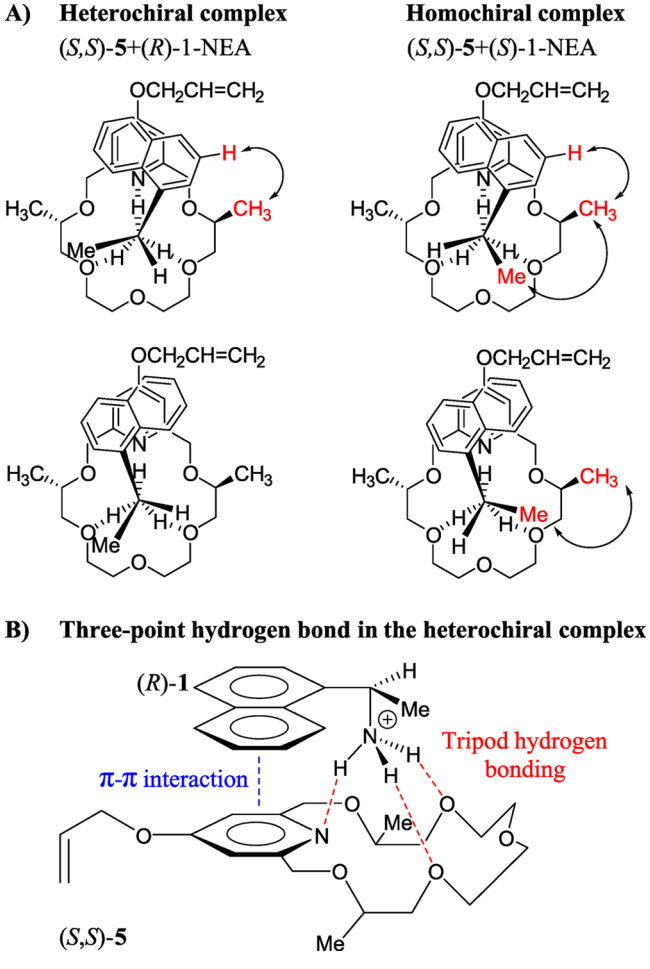

Figure 3. A) The hetero- and homochiral complexes between (*S*,*S*)-**5** and 1-NEA guest molecule. B) Noncovalent bonding of protonated primary aralkylamine enantiomers (template, (*R*)-**1**) with the pyridino-18-crown-6 ether derivative [functional monomer, (*S*,*S*)-**5**]: tripod hydrogen bonding and $\pi-\pi$ interactions.

while in case (iii) steric repulsion allows the formation of imprinted cavities with complementary chirality to the enantiopure template used. The aim of the present study is to test these hypotheses and explore the factors influencing the chiral recognition behavior of imprinted polymers featuring macrocyclic units.

In order to study the effect of ring size, chirality of the macrocycle and the presence of the pyridine subunit, three crown ether type functional monomers [(*S*,*S*)-**5**−**7**] and the corresponding precyclization analogues (**8** and **9**, Figure 2B) were synthesized. The uptake and release of the enantiomers of **1** by the imprinted polymers as well as their selectivity against protonated aralkylamines **2**, **3** and **4** were investigated.

The drug release from each IPs was analyzed using the five most often applied kinetic models, namely zero-order, first-order kinetics, Hixson−Crowell, Higuchi, and Korsmeyer−Peppas models.[13] When these models are used and analyzed in different polymers, the rate constant obtained from these models is an apparent rate constant. Controlled release of guests in pharmaceutical and food products is mainly described by zero-order or first-order kinetics.[14] The former expresses as extended release and the latter exhibits an immediate mode.[15]

RESULTS AND DISCUSSION

Design and Synthesis of Functional Monomer Anchors and Imprinted Polymers. Effective enantiomeric recognition

DOI: 10.1021/acsami.5b00755
ACS Appl. Mater. Interfaces 2015, 7, 9516−9525

with chiral macrocyclic receptors requires either C2, C3, or D2 symmetry.[6] Furthermore, the stability of the complexes can be increased by addition of electron donating groups to the aromatic subunit of the macrocycle (e.g., —OCH_3 or —$OCH_2CH{=}CH_2$).[6] Hence, we have chosen the pyridino-18-crown-6 ether (*S*,*S*)-**5** as functional monomer for the present study due to its favorable C2 symmetry and the allyloxy substituent. Commercially available (*S*)-ethyl lactate, diethyl oxalate, acetone, and sodium metal were used to prepare dimethyl substituted pyridono-18-crown-6 ether (*S*,*S*)-**10** in a multistep synthesis,[16] which was then reacted with allyl bromide in acetonitrile in the presence of Hünig's base to obtain functional monomer (*S*,*S*)-**5** in a good yield (Scheme 1). The earlier reported synthesis of this

Scheme 1. Synthesis of Functional Monomers (*S*,*S*)-5−9

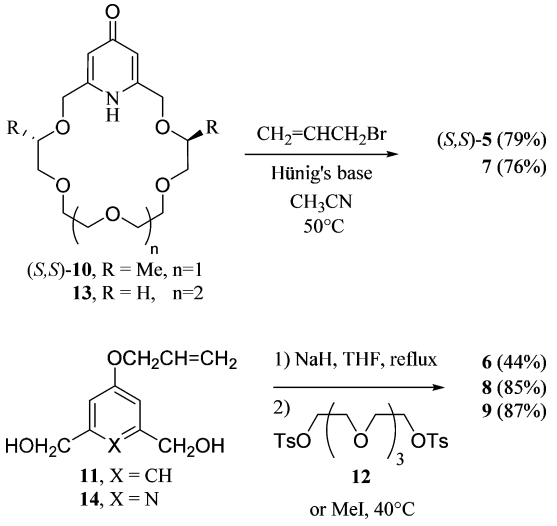

macrocycle[17] has been improved by changing the order of allylation and macrocyclization steps. Due to the sensitive nature of the allyloxy group it is advantageous to obtain (*S*,*S*)-**10** through the benzyloxy-pyridino-crown ether derivative and introduce the allyloxy group in the last step of the synthetic route. The latter synthesis gives a similar overall yield of about 20% and requires less tedious chromatographic purifications.

In order to investigate the effect of the nitrogen atom on complexation as well as the necessity of the chiral center for enantiomeric discrimination, the achiral benzo-18-crown-6 ether (**6**) analogue of (*S*,*S*)-**5** was synthesized (Scheme 1) and used as functional monomer for imprinting. The synthesis of **6** started with the conversion of the commercially available 5-hydroxyisophthalic acid to allyloxy diol **11**.[17] The latter was treated with sodium hydride in THF to gain the corresponding dialkoxide, which was then reacted with tetraethylene glycol ditosylate **12** performing a Williamson-type ether formation macrocyclization.

In order to study the effect of the size of the macroring to complexation 4-allyloxypyridino-21-crown-7 ether derivative **7** was synthesized in the same manner as the pyridino-18-crown-6 ether analogue (*S*,*S*)-**5** with the *O*-allylation[18] of the reported pyridono-21-crown-7 ether **13**[19] (Scheme 1).

The carbonyl moiety of ethane-1,2-diyl bis(2-methacrylate) (EDMA) cross-linker used for the preparation of the IPs can also donate electrons and thus contribute to the formation of a tripod hydrogen bonding similar to that of the macrocycle (Figure 3).

The precyclization analogues (**8**, **9**) of (*S*,*S*)-**5**, **6** and **7** were synthesized in order to show the significance of the macrocycle itself. The synthesis of functional monomers 4-allyloxy-2,6-bismethoxymethylpyridine (**8**) and its bismethoxymethyl-allyloxybenzene analogue (**9**) started from allyloxy diols **14** and **11** which were converted into the corresponding dialkoxides using sodium hydride in THF, followed by *O*-methylation with iodomethane (Scheme 1).

Heterochiral complexes have higher stability compared to that of homochiral complexes due to the stronger steric repulsion between the host and the guest (see Figure 3).[20] Given that functional monomer **5** has (*S*,*S*) configuration, the most stable heterochiral prepolymerization complex is formed with (*R*)-**1** enantiomer. In order to investigate the necessity of enantiopure template for IP fabrication two sets of imprinted polymers were prepared either in the presence of enantiopure [(*R*)-**1**] or racemic (Rac-**1**) template (Table 1). High functional monomer/

Table 1. Composition and Stoichiometry of the Imprinted Polymers and the Corresponding Control Polymers[a]

polymers	composition	stoichiometry
IP1[A]	(*R*)-**1**/(*S*,*S*)-**5**/EDMA	1/1/40
IP1[B]	Rac-**1**/(*S*,*S*)-**5**/EDMA	1/1/40
CP1	(*S*,*S*)-**5**/EDMA	1/40
IP2[A]	(*R*)-**1**/**6**/EDMA	1/1/40
IP2[B]	Rac-**1**/**6**/EDMA	1/1/40
CP2	**6**/EDMA	1/40
IP3[A]	(*R*)-**1**/**7**/EDMA	1/1/40
IP3[B]	Rac-**1**/**7**/EDMA	1/1/40
CP3	**7**/EDMA	1/40
IP4[A]	(*R*)-**1**/**8**/EDMA	1/1/40
IP4[B]	Rac-**1**/**8**/EDMA	1/1/40
CP4	**8**/EDMA	1/40
IP5[A]	(*R*)-**1**/**9**/EDMA	1/1/40
IP5[B]	Rac-**1**/**9**/EDMA	1/1/40
CP5	**9**/EDMA	1/40

[a]AIBN (azabisisobutyronitrile) was used as a radical initiator and acetonitrile/methanol (1/4) was used as porogen.

cross-linker ratio (1/40) was set resulting in highly cross-linked, robust polymeric networks. Elemental microanalysis of the polymers after extraction confirmed (i) the stoichiometrical incorporation of monomers into the polymers; (ii) the chemical identity of the imprinted and corresponding control polymers; and (iii) the successful removal of the template from the polymers.

Figure 4 shows typical scanning electron micrographs (SEM) of the obtained polymers having spherical uniformly sized particles with a size range of 40−60 μm, which is suitable for chromatographic stationary phase and solid-phase extraction. The capacity and enantioselectivity of the polymers were probed against the control polymers lacking the template during their preparation.

Enantioseparation Performance of the Polymers. The utilization of functional monomers can be assessed by relating the maximum number of binding sites (B_{max} = 200 μmol·g^{-1} of polymer) to the amount of analyte bound to the polymer, i.e., uptake of **1**. During the batch rebinding studies, both the imprinted and control polymers were loaded with a feed solution corresponding to B_{max} (20 mL of 20 mM Rac-**1** in acetonitrile/methanol (1/4) per gram of polymer was loaded) and Figure 5 summarizes the binding of **1**. Parameters such as binding (B), imprinting factor (IF), enantioseparation factor (EF), and selectivity factor (SF) were used to assess the performance of

DOI: 10.1021/acsami.5b00755
ACS Appl. Mater. Interfaces 2015, 7, 9516−9525

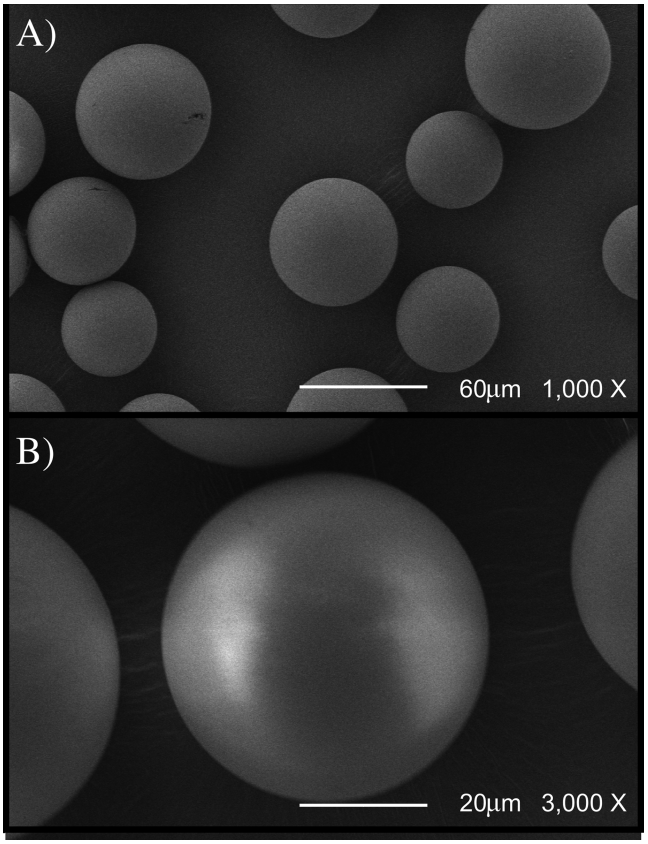

Figure 4. Typical SEM images of the IP particles of 1000 (A) and 3000 (B) magnification.

the polymers. Given that the adsorption isotherms of IPs are nonlinear, it is important to note that comparison of IP performance based on IF, EF, and SF values is strictly for qualitative purposes, as they are calculated at a single concentration of the enantiomers.[21] B is the bound concentration to feed concentration ratio as defined in eq 1:

$$B = \frac{c^{i}_{\text{Bound}}}{c^{i}_{\text{Feed}}} \tag{1}$$

where c^{i}_{Bound} and c^{i}_{Feed} are the bound concentration of compound i in equilibrium and feed concentration of compound i, respectively. IF is a useful measure of the effect of the presence of a template during polymerization on the performance of the scavengers, and it is defined in eq 2:

$$\text{IF} = \frac{B^{\text{IP}}_{(R)\text{-}1}}{B^{\text{CP}}_{(R)\text{-}1}} \tag{2}$$

where $B^{\text{IP}}_{(R)\text{-}1}$ and $B^{\text{CP}}_{(R)\text{-}1}$ are the bound concentration of (*R*)-**1** on the imprinted and the corresponding control polymer, respectively. EF allows the comparison of chiral discrimination power of different polymers and is defined in eq 3:

$$\text{EF} = \frac{B_{(R)\text{-}1}}{B_{(S)\text{-}1}} \tag{3}$$

where $B_{(R)\text{-}1}$ and $B_{(S)\text{-}1}$ represent the binding of (*R*)-**1** and (*S*)-**1** on the polymers, respectively.

Figure 5 demonstrates that macrocyclic units play a key role in the binding of quaternary ammonium salts. IP1 and IP2 derived from enantiopure (*S*,*S*)-**5** and achiral **6** macrocyclic functional monomers exhibit about 10 times higher binding of (*R*)-**1** than IP4 and IP5 derived from their precyclization analogues **8** and **9**, respectively. The binding of (*R*)-**1** on IP1 and IP2 is 97 and 81% corresponding to 194 and 162 μmol·g^{-1} of polymer, respectively. The molecular recognition performance of IP1 featuring enantiopure crown ether anchor is independent of the chiral nature of the template during polymerization. Hence, it is not necessary to use an enantiopure template as both the (*R*)-**1** and

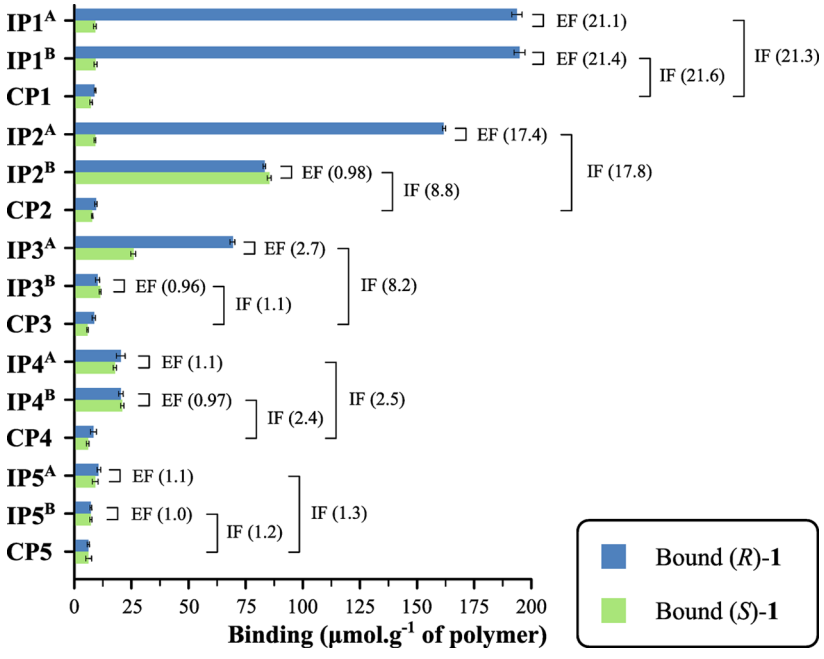

Figure 5. Binding of (*R*) and (*S*) enantiomers of **1** on the imprinted and control polymers. Enantioseparation factors (EF) and imprinting factors (IF) obtained are given for each enantiomer and polymer pairs, respectively. Twenty mL of 20 mM Rac-**1** in acetonitrile/methanol (1/4) per gram of polymer was loaded.

DOI: 10.1021/acsami.5b00755
ACS Appl. Mater. Interfaces 2015, 7, 9516−9525

Rac-**1** templated IPs exhibit (i) the same binding value of about 97% and (ii) the same enantioseparation factor of about 21 (Figure 5).

This phenomenon is in line with the previous observations about the complexing ability of crown ethers. Heterochiral complexes of enantiomerically pure pyridino crown ethers (i.e., (*R*,*R*)-crown ether-(*S*)-aralkylammonium salt and (*S*,*S*)-crown ether-(*R*)-aralkylammonium salt) exhibit higher stability compared to that of homochiral complexes (i.e., (*R*,*R*)-crown ether-(*R*)-aralkylammonium salt and (*S*,*S*)-crown ether-(*S*)-aralkylammonium salt).[20,22] Notice that the IP1 series have superior performance over all the other polymers regarding both enantioseparation and binding capacity.

The macrocyclic anchor of IP2 series is achiral and has benzene ring instead of pyridine. The benzo-18-crown-6 ether derivatives form less stable complexes with protonated primary aralkylamines,[18] thus IP2 has reduced binding capacity compared to IP1. Furthermore, achiral macrocycles have no chiral discrimination power and thus have the same affinity toward any (*R*) and (*S*) enantiomers. Hence, IP2^{B} prepared in the presence of Rac-**1** template does not show any discrimination between the enantiomer pair and they are both bound at the same level of about 85 μmol·g^{-1} of polymer (Figure 5). However, IP2^{A} prepared in the presence of (*R*)-**1** template is capable of enantiomerseparation. Since achiral functional monomer was used for the preparation of IP2, the enantiopure template induced the formation of a chiral binding site within the polymer network resulting in an enantiomerseparation factor of as high as 17. Furthermore, the size of the macroring also influences the complexing ability of the macrocycle and subsequently the performance of the imprinted polymers. 18-Crown-6 ethers form stronger complexes with guest primary alkylammonium cations than the analogous 21-membered hosts.[23] Hence, the binding capacity of IP3^{A} significantly declined (50%) compared with the corresponding 18-crown-6 derived IP2^{A} series (Figure 5). The IP4 and IP5 series featuring precyclization analogues of the crown ether anchors show neither appreciable imprinting nor enantioseparation factors. It has been demonstrated that the presence of the macrocycle is essential for the effective binding of protonated primary aralkylamines. Due to the overall superior performance, IP1 and IP2 series were further characterized by selectivity tests, adsorption isotherms and binding kinetics.

During the preparation of IPs an impression of the template is molded into the backbone of the growing polymer network, resulting in sought after high-fidelity binding sites.[24] The selectivity factor (SF) is used to describe the fidelity of the binding sites of the polymers and is defined in eq 4:

$$\mathrm{SF} = \frac{c_{(R)\text{-}1}}{c_i} \tag{4}$$

where $c_{(R)\text{-}1}$ and c_i are the bound concentration of (*R*)-**1** template and compound i in equilibrium on the polymers, respectively. Figure 6 demonstrates that both IP1 and IP2 series have high selectivity toward the (*R*)-**1** template over structurally similar protonated primary aralkylamines (Figure 2A).

The highest SF of about 35 was achieved by IP1 series, which is among the highest SFs achieved by IPs.[25] This can be explained by the formation of high-stability (*S*,*S*)-**5**−(*R*)-**1** heterochiral prepolymerization complexes, featuring a macrocycle with the adequate ring size capable of tripod hydrogen bonding and $\pi-\pi$ interaction,[20] under the mild polymerization conditions applied.

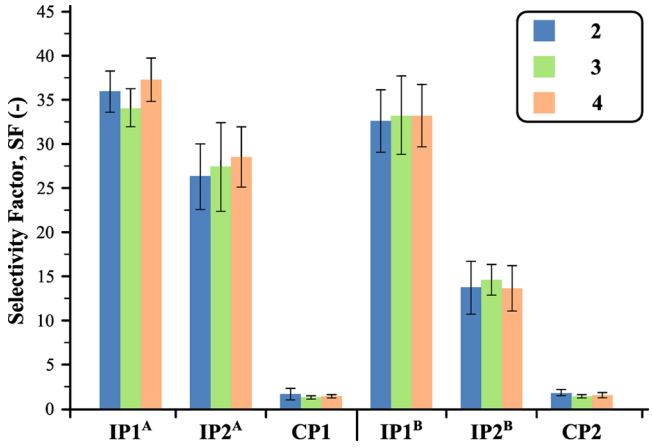

Figure 6. Selectivity factors of the imprinted and control polymers. Protonated primary aralkylamines **2**, **3**, and **4** were used to probe the selectivity of the polymers over the (*R*)-**1** template.

Adsorption Isotherms. The Langmuir and Freundlich are the most commonly used adsorption models and the former is defined in eq 5:

$$B = \frac{q_m k_a F}{1 + k_a F} \tag{5}$$

where B is the equilibrium concentration of (*R*)-**1** bound by the polymer, F is the free equilibrium concentration of (*R*)-**1**, k_a is the affinity constant, and q_m is the binding site density. It has been generally observed that the Langmuir model is more suitable than the Freundlich model for describing the adsorption process of ion-imprinted polymers having a macrocyclic anchor.[26]

The adsorption data obtained are best fit with the Langmuir model, indicating that the adsorption of (*R*)-**1** ions on both IPs and CPs is homogeneous. Table 2 shows the Langmuir isotherm constants for IP1 and IP2 series and the corresponding CPs toward (*R*)-**1**. Twenty mL of 6−12 mM Rac-**1** in acetonitrile/methanol (1/4) per gram of polymer was loaded and a typical isotherm fitted to the Langmuir model is shown in the Supporting Information (SI Figure S1).

Table 2. Langmuir Isotherm Constants for (*R*)-1 Adsorption on the Imprinted and Corresponding Control Polymers: Binding Capacity (q_m), Affinity Constant (k_a) and Binding Site Density ($q_m \times k_a$)[a]

polymers	q_m (mg·g^{-1})	k_a (L·mg^{-1})	$q_m \times k_a$ (L·g^{-1})	R^2
IP1^{A}	60.1 ± 0.3	0.100 ± 0.012	6.02 ± 0.72	0.9993
IP1^{B}	59.7 ± 0.3	0.081 ± 0.007	4.85 ± 0.39	0.9997
CP1	2.7 ± 0.3	0.005 ± 0.003	0.01 ± 0.01	0.9996
IP2^{A}	47.3 ± 0.2	0.040 ± 0.002	1.89 ± 0.10	0.9994
IP2^{B}	23.9 ± 0.4	0.013 ± 0.002	0.30 ± 0.04	0.9997
CP2	2.7 ± 0.1	0.005 ± 0.001	0.01 ± 0.01	0.9994

[a]20 mL of 6−12 mM Rac-**1** in acetonitrile/methanol (1/4) per gram polymer was loaded.

The maximum adsorption capacities (q_m) are an order of magnitude higher for the imprinted polymers than for the control polymers, indicating that IPs have a stronger affinity and more adsorption sites for (*R*)-**1** than CPs. The highest adsorption capacity of about 60 mg.g^{-1} is achieved by IP1 series featuring pyridine functionality. Furthermore, the adsorption capacity of IP1^{A} and IP1^{B} is virtually the same, confirming that the use of

DOI: 10.1021/acsami.5b00755
ACS Appl. Mater. Interfaces 2015, 7, 9516−9525

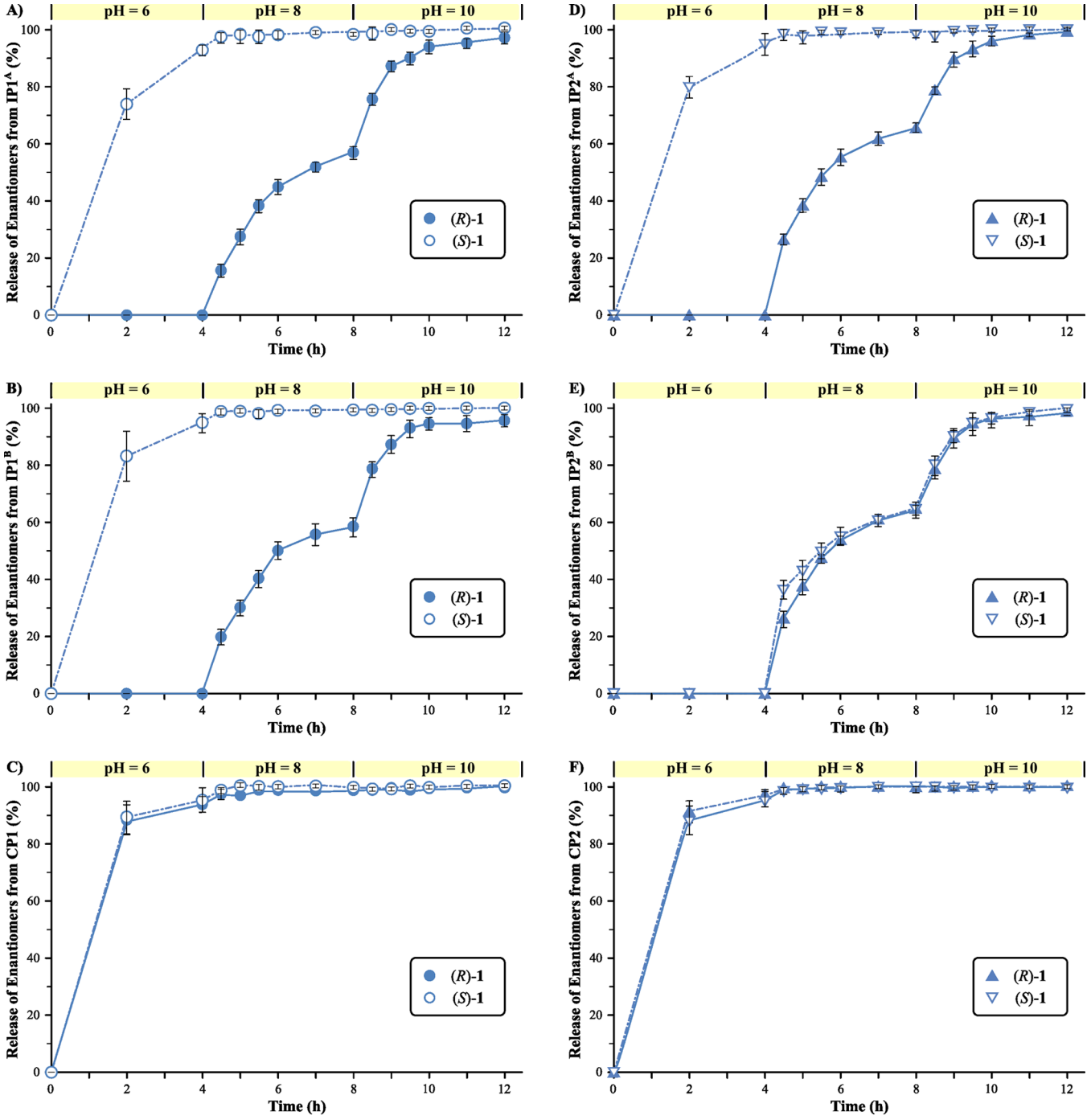

Figure 7. Release kinetic profile of **1** enantiomers from IP1 (A–B) and IP2 (D–E) series and from the corresponding control polymers (C, F) in response to pH stimuli. The release amount is expressed as the percentage of **1** released toward the total **1** uptake by the polymers. Twenty mL of 20 mM Rac-**1** in water per gram of polymer was loaded at pH = 6 which was increased to pH = 8 and pH = 10 after 4 and 8 h, respectively.

racemic template is sufficient to achieve enantioseparation when enantiopure macrocyclic anchor is employed. Due to the lack of pyridine ring in the macrocyclic anchor the $IP2^A$ and $IP2^B$ have 22% and 60% lower adsorption capacity than the IP1 series, respectively.

In Vitro Controlled Drug Release Experiments and Pharmaceutical Cleanup. Polymers have gained importance in the pharmaceutical industry as both drug encapsulants and vehicles for drug carriage, either protecting an active pharmaceutical ingredient (API) or controlling its release. The application of molecular imprinting in the field of drug delivery can improve the control over the therapeutic release. IPs have been recently proposed for the development of enantioselective-controlled drug release systems,[27] and for API purification.[28] The effect of varying the pH was investigated toward the IPs performance as controlled drug delivery devices. Twenty mL of 20 mM Rac-**1** in water per gram of polymer was loaded at pH = 6 which was increased to pH = 8 and pH = 10 after 4 and 8 h, respectively. Figure 7 shows the in vitro release kinetic profiles of the enantiomer pair of **1** from the polymers as a function of time and pH. Figure 7 demonstrates that the release rate of the template (*R*)-**1** enantiomer from the IP1 series and $IP2^A$ is highly

DOI: 10.1021/acsami.5b00755
ACS Appl. Mater. Interfaces 2015, 7, 9516–9525

pH-dependent, while the (*S*)-**1** release is nearly instantaneous regardless of pH. However, both enantiomers of **1** have the same, pH-dependent release profiles on IP2^B due to the lack of chiral discrimination power of this particular IP (lacking a chiral anchor and prepared in the presence of racemic **1**). This phenomenon is in line with the previous observations regarding uptake of enantiomers of **1**, showing an EF value of 0.98 (Figure 5). Under slightly acidic conditions (*R*)-**1** was fully retained by all the IP vehicles. However, the increase of pH above the pK_a value of **1** (pK_a = 9.26) allowed quasi quantitative release of the analyte due to excessive deprotonation of 1 and subsequent termination of the tripod hydrogen bonding host–guest system (see Figure 2). On the other hand, >90% of the (*S*)-**1** was released within 2 h at pH = 6, suggesting that the (*S*) enantiomer is only bound to the bulk of the polymer matrix rather than to the macrocyclic anchor. Besides the imprinting effect, the observed difference in the release rate of IPs and CPs could be explained by the lower pore volume and surface area of the particles (Table 3) that are less advantageous to analyte impregnation within the pores and with the analyte being retained more on the surface, which is responsible for the rapid initial release.

Table 3. Physical Characteristics (Surface Area, Average Pore Diameter and Specific Pore Volume) of IP1^A, IP2^A, IP1^B, IP2^B, and the Corresponding Control Polymers, Obtained by Multipoint BET Method

polymers	surface area ($m^2 \cdot g^{-1}$)	pore volume ($cm^3 \cdot g^{-1}$)	pore size (nm)
IP1^A	73.0 ± 2.0	0.124 ± 0.01	6.80 ± 0.02
IP1^B	71.2 ± 2.0	0.120 ± 0.02	6.82 ± 0.05
CP1	33.9 ± 4.3	0.058 ± 0.01	6.89 ± 0.01
IP2^A	72.8 ± 1.9	0.125 ± 0.01	6.86 ± 0.08
IP2^B	70.7 ± 8.1	0.122 ± 0.01	6.88 ± 0.02
CP2	44.6 ± 6.6	0.077 ± 0.01	6.87 ± 0.02

The insight into the uptake and release of **1** revealed that the careful adjustment of pH enables to enrich and control the release of the (*R*)-**1** enantiomer from the imprinted matrices. The pH dependence release could be further exploited for API purification. A schematic for the operation of racemic drug-loaded IP particles illustrates this point in Figure 8.

After the enrichment (API purification) of the (*R*) enantiomer, the particles can be used as drug carriers. pH-Sensitive drug delivery systems are gaining importance, as they deliver the APIs at specific time as per the pathophysiological need of the disease, resulting in improved patient therapeutic efficacy and compliance.[29] The amine functionality of template (*R*)-**1** remains protonated in the acidic and neutral environment of the stomach and the small intestine, thus the particle retains and protects the loaded drug. Whereas in alkaline environments of the small intestine, the amine groups become deprotonated and release the loaded drug molecules into the surrounding medium. The general concept of enantiomeric enrichment and pH-sensitive drug release described above should be extendable to other classes of chiral API salts.

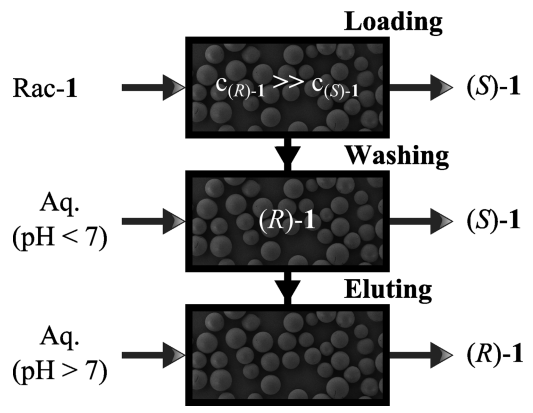

Figure 8. Schematic drawing of enhanced enantioseparation by controlled pH stimuli.

Given that the best enantioseparation performance was achieved with IP1 and IP2 polymers (see Figure 5) their release kinetics were further studied. The five most common kinetic models, namely zero order kinetics (eq 7), first order kinetics (eq 8), Higuchi model (eq 9), Hixson–Crowell model (eq 10), and Korsmeyer–Peppas model (eq 11) were applied:[30]

$$F = F_0 + k_0 t \tag{7}$$

$$\ln(1 - F) = k_1 t \tag{8}$$

$$F = k_2 t^{1/2} \tag{9}$$

$$(1 - F)^{1/3} = 1 - k_3 t \tag{10}$$

$$F = k_4 t^n \tag{11}$$

where F_0 and F represent the initial fraction and fraction of template released at time t, respectively, whereas k_0, k_1, k_2, k_3, and k_4 are the zero-order release constant, the first-order release constant, the Higuchi dissolution constant, the Hixson–Crowell release constant and the Korsmeyer–Peppas constant incorporating the structural and geometric characteristics of the IP dosage form, respectively. n is the release exponent, indicative of the template release mechanism. The fitting results for all polymers applying the five kinetics models are summarized in the SI (Table S1).

Release kinetic data obtained for the majority of both imprinted and control polymers were best fitted with the first-order model (SI Table S1). First-order model serves immediate mode of drug release and indicates that the rate limiting step for release is diffusion and it is not strongly concentration dependent. This is one the most often occurring kinetics in drug delivery. It can be concluded that under the same conditions the higher the pH value is, the higher the value of rate constants k_1, k_3, k_4 are, and the lower the value of rate constant k_2 becomes. Investigation of the kinetic models reaffirmed that the faster drug release in basic media is mainly due to the incremental deprotonation of **1**.

CONCLUSIONS

Three pyridine and two benzene based macrocycles containing allyloxy moiety [(*S*,*S*)-**5**, **6**–**7**] and their precyclization analogues (**8** and **9**) have been synthesized and evaluated as functional monomers for the recognition of enantiomers by molecular imprinting. Allyloxy group was chosen to introduce a polymerizable moiety due to its electron donating ability increasing the complexation stability. A facile way of purifying dimethyl-substituted (*S*,*S*)-**5** pyridino-crown ether was demonstrated via changing the order of the allylation and the macrocyclization steps of its synthesis. The presence of the macrocycle led to significant improvement with regards to capacity and selectivity. The performance of the imprinted polymers is highly dependent on the functionality and size of the macrocycle and the chiral

DOI: 10.1021/acsami.5b00755
ACS Appl. Mater. Interfaces 2015, 7, 9516–9525

nature of the template, and less dependent on the chiral nature of the macrocylic anchor. The polymers featuring enantiomerically pure macrocyclic anchor (*S*,*S*)-**5** provided imprinting and enantioseparation factors as high as 21 and 17, respectively, regardless of the enantiomeric purity of template **1**. However, achiral macrocyclic anchor necessitates the use of enantiomerically pure template in order to achieve enantiomeric discrimination. Furthermore, it has been demonstrated that the incorporation of a pyridine ring into the macrocycle enhances the adsorption capacity of the polymer up to 60%. The application of macrocyclic anchors resulted in high-fidelity binding sites providing selectivity factors as high as 35. Furthermore, selective release of the (*R*)-**1** from the IP vehicles in response to pH stimuli was observed. In vitro drug delivery showed that imprinted polymers released the drug in a more sustained way than the corresponding control matrices. It has been demonstrated that the polymers respond to pH stimuli allowing the improvement of enantioseparation performance by selective washing of (*S*)-**1** under acidic conditions, followed by the selective elution of (*R*)-**1** enantiomer. Applications as drug carriers in which release is controlled by a stimulus, such as the varying pH present in the intestinal tract, are envisaged. Kinetic studies revealed the mode of release to be first order and thus the IPs can serve immediate drug release at basic pH. Moreover, the IPs can be used for enrichment of chiral drugs.

The macrocycle assisted imprinting approach for enantioseparation of protonated primary aralkylamines has been successfully demonstrated. The general concepts described above should be extendable to other classes of macrocycles and enantiomers, and could be applied in chiral resolution of drugs, enantioselective sensors and pH-responsive drug delivery systems.

EXPERIMENTAL SECTION

General. Infrared spectra were recorded on a Bruker Alpha-T FT−IR spectrometer. Optical rotations were taken on a PerkinElmer 241 polarimeter that was calibrated by measuring the optical rotations of both enantiomers of menthol. NMR spectra were recorded in $CDCl_3$ either on a Bruker DRX-500 Avance spectrometer (at 500 MHz for ^1H and at 125 MHz for ^{13}C spectra) or on a Bruker 300 Avance spectrometer (at 300 MHz for ^1H and at 75 MHz for ^{13}C spectra) as specified for each compound. Mass spectra were recorded on Micromass LCT Premier (ESI) mass spectrometers. The nitrogen sorption measurements were performed on a Quantachrome Autosorb 6B automatic adsorption instrument. Rebinding, selectivity and release samples were analyzed by a High Performance Liquid Chromatograph (HPLC) Agilent model 1100 Series system using the method reported by Kupai et al.[22] Reagents were purchased from Sigma-Aldrich Ltd. and used as supplied, except where specified. EDMA was washed with 1 M aqueous NaOH and dried over Na_2SO_4 and distilled under vacuum prior to use. All solvents were analytical grades and dried with molecular sieves to eliminate traces of water before use. Elemental analyses were performed in the Microanalytical Laboratory of the Department of Organic Chemistry, Institute for Chemistry, L. Eötvös Loránd University, Budapest, Hungary. Starting materials were purchased from Aldrich Chemical Co., unless otherwise noted. Silica gel 60 F_{254} (Merck) and aluminum oxide 60 F_{254} neutral type E (Merck) plates were used for TLC. Aluminum oxide (neutral, activated, Brockman I) and silica gel 60 (70−230 mesh, Merck) were used for column chromatography. Ratios of solvents for the eluents are given in volumes (mL/mL). Solvents were dried and purified according to well established methods. Evaporations were carried out under reduced pressure unless otherwise stated.

Preparation and Characterization of Functional Monomers. (4*S*,14*S*)-(+)-19-Allyloxy-4,14-dimethyl-3,6,9,12,15-pentaoxa-21-azabicyclo[15.3.1]heneicosa-1(21),17,19-triene [(*S*,*S*)-5]. To a solution of dimethyl-substituted pyridono-crown ether (*S*,*S*)-**10** (269.0 mg, 0.79 mmol) in pure and dry acetonitrile (12 mL) was added first Hünig's base (1.14 mL, 844 mg, 6.54 mmol) followed by allyl bromide (375 μL, 675 mg, 5.3 mmol), and the resulting mixture was stirred at 50 °C until the TLC analysis (alumina TLC; EtOH−toluene 1:20) showed the total consumption of the starting material (R_f = 0.20) and only one main spot (R_f = 0.62) for the product (8 h). The volatile components were removed and the residue was dissolved in a mixture of DCM (50 mL) and water (50 mL). The aqueous layer was extracted with DCM (3 × 30 mL). The combined organic phase was dried over $MgSO_4$, filtered and the solvent was evaporated. The crude product was purified by column chromatography on neutral aluminum oxide using EtOH−toluene (1:80) mixture as an eluent to gain (*S*,*S*)-**5** (238.5 mg, 79%) as a pale yellow oil. R_f = 0.62 (alumina TLC, EtOH−toluene =1:20). $[\alpha]_D^{25}$= +26.4 (c 1.50 in $CHCl_3$); IR (neat) ν_{max} 3084, 1596, 1576, 1449, 1374, 1107, 1041 cm^{-1}; ^1H NMR (500 MHz, $CDCl_3$) δ (ppm) 1.15 (d, 6H, CH_3), 3.41−3.62 (m, 12H, OCH_2), 3.73−3.88 (m, 2H, $OCHCH_3$), 4.57−4.59 (m, 2H, $OCH_2CH{=}CH_2$), 4.69−4.78 (m, 4H, benzylic CH_2), 5.28−5.32 (m, 1H, $OCH_2CH{=}CH_2$), 5.38−5.44 (m, 1H, $OCH_2CH{=}CH_2$), 5.97−6.06 (m, 1H, $OCH_2CH{=}CH_2$), 6.79 (s, 2H, Pyr CH); ^{13}C NMR (125 MHz, $CDCl_3$) δ (ppm) 17.30 (CH_3), 68.64 ($OCH_2CH{=}CH_2$), 70.79 (OCH_2), 70.94 (OCH_2), 71.97 (OCH_2), 73.80 (OCH_2), 76.12 (OCH_2), 107.05 (Pyr-C), 118.45 ($OCH_2CH{=}CH_2$), 132.40 ($OCH_2CH{=}CH_2$), 160.47 (Pyr-C), 165.58 (Pyr-C); MS: 382.2221 $(M+1)^+$; Anal. Calcd for $C_{20}H_{31}NO_6$: C, 62.97; H, 8.19; N, 3.67. Found: C, 62.88; H, 7.92; N, 3.65.

19-Allyloxy-3,6,9,12,15-pentaoxabicyclo[15.3.1]heneicosa-1(21),17,19-triene (6). In a dry three-necked round-bottom flask equipped with a reflux condenser, argon inlet, and a dropping funnel was stirred vigorously a suspension of NaH (34.5 mg, 0.86 mmol, 60% dispersion in mineral oil) in pure and dry THF (1 mL) at 0 °C for 2 min. To this suspension was added slowly allyloxy diol **11** (59.7 mg, 0.31 mmol) dissolved in pure and dry THF (1 mL) under argon at 0 °C. The reaction mixture was stirred at 0 °C for 10 min, at room temperature for 30 min and at reflux temperature for 4 h. The mixture was cooled down to −20 °C and tetraethylene glycol ditosylate **12** (170.0 mg, 0.34 mmol) dissolved in pure and dry THF (1 mL) was added in 0.5 h. After addition of the ditosylate the reaction mixture was allowed to warm up slowly to room temperature and it was stirred at this temperature until the TLC analysis (alumina TLC; EtOH−toluene 1:100) showed the total consumption of the starting materials and only one main spot (R_f =0.44) for the product (2 days). The solvent was evaporated, and the residue was dissolved in a mixture of Et_2O and ice−water (10 mL of each). The phases were shaken thoroughly and separated. The aqueous phase was extracted with CH_2Cl_2 (3 × 10 mL). The combined organic phase was dried over anhydrous $MgSO_4$, filtered and evaporated. The crude product was purified by column chromatography on neutral aluminum oxide using EtOH−toluene (1:250) mixture as an eluent to gain **6** (47.7 mg, 44%) as a pale yellow oil. R_f: 0.44 (alumina TLC, EtOH−toluene = 1:100). IR (neat) ν_{max} 2862, 1648, 1598, 1450, 1351, 1324, 1292, 1258, 1200, 1100, 1020, 930, 858, 793, 714, 697, 660, 643, 549 cm^{-1}; ^1H NMR (300 MHz, $CDCl_3$) δ (ppm) 3.66−3.71 (m, 16H, OCH_2), 4.53−4.54 (m, 2H, $OCH_2CH{=}CH_2$), 4.61 (s, 4H, benzylic CH_2), 5.26−5.30 (m, 1H, $OCH_2CH{=}CH_2$), 5.38−5.44 (m, 1H, $OCH_2CH{=}CH_2$), 5.99−6.12 (m, 1H, $OCH_2CH{=}CH_2$), 6.71 (s, 2H, Ar—CH), 7.32 (s, 1H, Ar—CH); ^{13}C NMR (75.5 MHz, $CDCl_3$) δ (ppm) 68.84 ($OCH_2CH{=}CH_2$), 69.33 (OCH_2), 70.79 (OCH_2), 70.80 (OCH_2), 70.99 (OCH_2), 72.76 (OCH_2), 112.73 (Ar—CH), 117.63 ($OCH_2CH{=}CH_2$), 119.10 (Ar—CH), 133.29 ($OCH_2CH{=}CH_2$), 140.32 (Ar—CH), 158.59 (Ar—CH); MS: 370.2000 $(M+H_2O)$; Anal. Calcd for $C_{19}H_{28}O_6.H_2O$: C, 61.60; H, 8.16. Found: C, 61.52; H, 8.19.

22-Allyloxy-3,6,9,12,15,18-hexaoxa-24-azabicyclo [18.3.1]-tetracosa-20,22,24-triene (7). To a solution of pyridono-crown ether **13** (789.8 mg, 2.21 mmol) in pure and dry acetonitrile (8 mL) was added first Hünig's base (640 μL, 474 mg, 3.67 mmol) followed by allyl bromide (210 μL, 294 mg, 2.43 mmol), and the resulting mixture was stirred at 50 °C until the TLC analysis (alumina TLC; EtOH−toluene 1:10) showed only one main spot (R_f = 0.71) for the product (4 h). The volatile components were removed and the residue was dissolved in a mixture of DCM (50 mL) and water (50 mL). The aqueous layer was extracted with DCM (2 × 50 mL). The combined organic phase was

DOI: 10.1021/acsami.5b00755
ACS Appl. Mater. Interfaces 2015, 7, 9516−9525

dried over $MgSO_4$, filtered and the solvent was evaporated. The crude product was purified by column chromatography on neutral aluminum oxide using EtOH−toluene (1:100) mixture as an eluent to yield **7** (667.6 mg, 76%) as a pale yellow oil. R_f: 0.71 (alumina TLC, EtOH−toluene =1:10). IR (neat) ν_{max} 2863, 1653, 1647, 1636, 1624, 1597, 1576, 1560, 1449, 1351, 1323, 1297, 1250, 1102, 1041, 989, 935, 859, 702, 599, 571, 556, 539, 530 cm^{-1}; ^1H NMR (300 MHz, $CDCl_3$) δ (ppm) 3.56 (s, 12H, OCH_2), 3.64−3.65 (m, 4H, OCH_2), 3.70−3.73 (m, 4H, OCH_2), 4.56−4.58 (m, 2H, $OCH_2CH{=}CH_2$), 4.62 (s, 4H, benzylic CH_2), 5.26−5.30 (m, 1H, $OCH_2CH{=}CH_2$), 5.36−5.41 (m, 1H, $OCH_2CH{=}CH_2$), 5.94−6.06 (m, 1H, $OCH_2CH{=}CH_2$), 6.83 (s, 2H, Pyr CH); ^{13}C NMR (75.5 MHz, $CDCl_3$) δ (ppm) 68.63 ($OCH_2CH{=}CH_2$), 69.94 (OCH_2), 70.71 (OCH_2), 70.88 (OCH_2), 70.92 (OCH_2), 70.97 (OCH_2), 74.12 (OCH_2), 107.53 (Pyr-C), 118.35 ($OCH_2CH{=}CH_2$), 132.28 ($OCH_2CH{=}CH_2$), 159.79 (Pyr-C), 166.00 (Pyr-C); MS: 398.2176 $(M+1)^+$; Anal. Calcd for $C_{20}H_{31}NO_7$: C, 60.44; H, 7.86; N, 3.52. Found: C, 60.41; H, 7.90; N, 3.48.

4-(Allyloxy)-2,6-bis(methoxymethyl)pyridine (8). In a dry three-necked round-bottom flask equipped with a reflux condenser, argon inlet and a dropping funnel was stirred vigorously a suspension of NaH (49.8 mg, 1.24 mmol, 60% dispersion in mineral oil) in pure and dry THF (2 mL) at 0 °C for 2 min. To this suspension was added slowly allyloxy diol **14** (110.3 mg, 0.565 mmol) dissolved in pure and dry THF (2 mL) under argon at 0 °C. The reaction mixture was stirred at 0 °C for 10 min, at room temperature for 30 min and at reflux temperature for 1 h. The mixture was cooled down to 10 °C and MeI (78 μL, 176.4 mg, 1.24 mmol) dissolved in pure and dry THF (2 mL) was added in 5 min. After addition of the alkylation reagent the reaction mixture was allowed to warm up slowly to room temperature and it was stirred under these conditions until the TLC analysis (SiO_2 TLC; MeOH−toluene 1:4) showed the total consumption of the starting materials (4 h). The solvent was evaporated, and the residue was dissolved in a mixture of Et_2O and ice−water (20 mL of each). The phases were shaken thoroughly and separated. The aqueous phase was extracted with Et_2O (3 × 20 mL). The combined organic phase was dried over anhydrous $MgSO_4$, filtered and evaporated. The crude product was purified by column chromatography on neutral silica gel using MeOH−toluene (1:8) mixture as an eluent to gain **8** (107.1 mg, 85%) as a pale yellow oil. R_f: 0.39 (silica TLC, MeOH−toluene =1:4).; IR (neat) ν_{max} 2928, 2877, 2820, 1597, 1578, 1448, 1426, 1389, 1354, 1317, 1288, 1247, 1191, 1159, 1110, 1044, 978, 925, 861, 845 cm^{-1}; ^1H NMR (500 MHz, $CDCl_3$) δ (ppm) 3.45 (s, 6H, CH_3), 4.50 (s, 4H, benzylic CH_2), 4.59−4.61 (m, 2H, $OCH_2CH{=}CH_2$), 5.29−5.31 (m, 1H, $OCH_2CH{=}CH_2$), 5.38−5.42 (m, 1H, $OCH_2CH{=}CH_2$), 5.98−6.05 (m, 1H, $OCH_2CH{=}CH_2$), 6.86 (s, 2H, Pyr CH); ^{13}C NMR (75.5 MHz, $CDCl_3$) δ (ppm) 58.92 (CH_3), 68.72 ($OCH_2CH{=}CH_2$), 75.42 (benzylic CH_2), 106.53 (Pyr-CH), 118.44 ($OCH_2CH{=}CH_2$), 132.19 ($OCH_2CH{=}CH_2$), 159.85 (Pyr-CH), 166.39 (Pyr-CH); MS: 224.1293 $(M+1)^+$; Anal. Calcd for $C_{12}H_{17}NO_3$: C, 64.55; H, 7.67; N, 6.27. Found: C, 64.39; H, 7.74; N, 6.19.

1-(Allyloxy)-3,5-bis(methoxymethyl)benzene (9). In a dry three-necked round-bottom flask equipped with a reflux condenser, argon inlet and a dropping funnel was stirred vigorously a suspension of NaH (135.4 mg, 3.38 mmol, 60% dispersion in mineral oil) in pure and dry THF (5 mL) at 0 °C for 2 min. To this suspension was added slowly allyloxy diol **11** (298.7 mg, 1.54 mmol) dissolved in pure and dry THF (5 mL) under argon at 0 °C. The reaction mixture was stirred at 0 °C for 10 min, at room temperature for 30 min and at reflux temperature for 1 h. The mixture was cooled down to 10 °C and MeI (215 μL, 480.2 mg, 3.38 mmol) dissolved in pure and dry THF (5 mL) was added in 5 min. After addition of the alkylation reagent the reaction mixture was allowed to warm up slowly to room temperature, and it was stirred under these conditions until the TLC analysis (SiO_2 TLC; MeOH−toluene 1:8) showed the total consumption of the starting materials (4 h). The solvent was evaporated, and the residue was dissolved in a mixture of Et_2O and ice−water (25 mL of each). The phases were shaken thoroughly and separated. The aqueous phase was extracted with Et_2O (3 × 25 mL). The combined organic phase was dried over anhydrous $MgSO_4$, filtered, and evaporated. The crude product was purified by column chromatography on neutral silica gel using MeOH−toluene (1:8) mixture as an eluent to gain **9** (297.4 mg, 87%) as a pale yellow oil. R_f: 0.82 (silica TLC, MeOH−toluene = 1:4); IR (neat) ν_{max} 2924, 2856, 2820, 1597, 1453, 1424, 1409, 1382, 1362, 1323, 1294, 1193, 1154, 1097, 1054, 993, 924, 843, 723, 689 cm^{-1}; ^1H NMR (300 MHz, $CDCl_3$) δ (ppm) 3.40 (s, 6H, CH_3), 4.44 (s, 4H, benzylic CH_2), 4.56−4.57 (m, 2H, $OCH_2CH{=}CH_2$), 5.27−5.31 (m, 1H, $OCH_2CH{=}CH_2$), 5.40−5.46 (m, 1H, $OCH_2CH{=}CH_2$), 6.01−6.14 (m, 1H $OCH_2CH{=}CH_2$), 6.86 (s, 2H, Ar—CH), 6.90 (s, 1H, Ar—CH); ^{13}C NMR (75.5 MHz, $CDCl_3$) δ (ppm) 58.18 (CH_3), 68.83 ($OCH_2CH{=}CH_2$), 74.50 (benzylic CH_2), 113.13 (Ar—CH), 117.56 (Ar−CH), 119.28 ($OCH_2CH{=}CH_2$), 133.31 ($OCH_2CH{=}CH_2$), 139.85 (Ar—CH), 159.08 (Ar—CH); MS: 223.1304 $(M+1)^+$; Anal. Calcd for $C_{13}H_{18}O_3$: C, 70.24; H, 8.16. Found: C, 70.12; H, 8.32.

Preparation of Molecularly Imprinted Polymers. IP microspheres were prepared by a suspension polymerization method according to the procedure established by Mayes and Mosbach.[31] Briefly, in a typical IP fabrication procedure the functional monomer (*S*,*S*)-**5**, **6**, **7**, **8**, and **9** (0.1 mmol), either enantiopure (*R*)-**1** or racemic **1** template (0.1 mmol), EDMA cross-linker (4 mmol), AIBN initiator (0.01 mmol), perfluoro polymeric surfactant (PFPS) emulsifier (15 mg), perfluoro methylcyclohexane (PMC) dispersing phase (12 mL) and methanol/acetonitrile (1/4) (2 mL) porogen were stirred at a constant rotation rate of 300 rpm. The IPs were obtained by polymerization involving the irradiation of the stirred mixture with UV light for 6 h at wavelength of 365 nm at room temperature under inert atmosphere. The resulting beads were filtered and the remaining template and unreacted molecules were extracted by sequential washing with 10 mM tetramethylammonium hydroxide (TMAH) in acetonitrile/methanol (1/4) followed by rinsing with acetonitrile. The IPs were dried under reduced pressure for 24 h at room temperature. The CPs were fabricated in the same procedure but no template molecule was included in the reaction mixture. Anal. Calcd/Found for extracted polymers: $IP1^A$ (C, 60.74/60.51; H, 7.17/7.08; N, 0.24/0.22), $IP1^B$ (C, 60.74/60.43; H, 7.17/7.05; N, 0.24/0.21), CP1 (C, 60.74/60.56; H, 7.17/7.11; N, 0.24/0.22), $IP2^A$ (C, 60.80/60.62; H, 7.16/7.12; N, 0.07/0.05), $IP2^B$ (C, 60.80/60.58; H, 7.16/7.07.; N, 0.07/0.05), CP2 (C, 60.80/60.48; H, 7.16/7.13; N, 0.07/0.04), $IP3^A$ (C, 60.62/60.67; H, 7.16/7.13; N, 0.23/0.25), $IP3^B$ (C, 60.62/60.60; H, 7.16/7.09; N, 0.23/0.21), CP3 (C, 60.62/60.54; H, 7.16/7.11; N, 0.23/0.22), $IP4^A$ (C, 60.74/60.53; H, 7.14/7.12; N, 0.24/0.23), $IP4^B$ (C, 60.74/60.58; H, 7.14/7.10; N, 0.24/0.22), CP4 (C, 60.74/60.46; H, 7.14/7.09; N, 0.24/0.22), $IP5^A$ (C, 60.89/60.72; H, 7.15/7.13; N, 0.07/0.05), $IP5^B$ (C, 60.89/60.69; H, 7.15/7.12; N, 0.07/0.08), CP5 (C, 60.89/60.63; H, 7.15/7.10; N, 0.07/0.08).

■ ASSOCIATED CONTENT

Supporting Information

Detailed syntheses of functional monomers; a typical isotherm fitted to the Langmuir model; IR Spectra of functional monomers; ^1H and ^{13}C NMR Facsimilies; ESI mass spectra; and fitting results for all polymers applying the five kinetics models. The Supporting Information is available free of charge on the ACS Publications website at DOI: 10.1021/acsami.5b00755.

■ AUTHOR INFORMATION

Corresponding Author

*Tel.: +44(0)161 306 4366; E-mail: gyorgy.szekely@manchester.ac.uk.

Notes

The authors declare no competing financial interest.

■ ACKNOWLEDGMENTS

Financial support of the Hungarian Scientific Research Fund (OTKA K81127 to P.H., PD108462 to J.K.) is gratefully acknowledged.

DOI: 10.1021/acsami.5b00755
ACS Appl. Mater. Interfaces 2015, 7, 9516−9525

ABBREVIATIONS

IP, imprinted polymer
EDMA, ethane-1,2-diyl bis(2-methacrylate)
SEM, scanning electron micrographs
AIBN, azabis(isobutyronitrile)
IF, imprinting factor
EF, enantioseparation factor
SF, selectivity factor
TLC, thin layer chromatography
API, active pharmaceutical ingredient
PFPS, perfluoro polymeric surfactant
PMC, perfluoro methylcyclohexane
TMAH, tetramethylammonium hydroxide

REFERENCES

(1) Wattanakit, C.; Come, Y. B.; Lapeyre, V.; Bopp, P. A.; Heim, M.; Yadnum, S.; Nokbin, S.; Warakulwit, C.; Limtrakul, J.; Kuhn, A. Enantioselective Recognition at Mesoporous Chiral Metal Surfaces. *Nat. Commun.* **2014**, *5*, 3325.

(2) Wulff, G.; Sarhan, A.; Zabrocki, K. Enzyme-Analogue Built Polymers and Their Use for the Resolution of Racemates. *Tetrahedron Lett.* **1973**, *44*, 4329−4332.

(3) Andersson, L.; Ekberg, B.; Mosbach, K. Synthesis of a New Amino Acid Based Cross-Linker for Preparation of Substrate Selective Acrylic Polymers. *Tetrahedron Lett.* **1985**, *26*, 3623−3624.

(4) Hosoya, K.; Yoshizako, K.; Shirasu, Y.; Kimata, K.; Araki, T.; Tanaka, N.; Haginaka, J. Molecularly Imprinted Uniform-Size Polymer-Based Stationary Phase for High-Performance Liquid Chromatography Structural Contribution of Cross-Linked Polymer Network on Specific Molecular Recognition. *J. Chromatogr. A* **1996**, *728*, 139−147.

(5) Hosoya, K.; Shirasu, Y.; Kazuhiro, K.; Tanaka, N. Molecularly Imprinted Chiral Stationary Phase Prepared with Racemic Template. *Anal. Chem.* **1998**, *70*, 943−945.

(6) Zhang, X. X.; Bradshaw, J. S.; Izatt, R. M. Enantiomeric Recognition of Amine Compounds by Chiral Macrocyclic Receptors. *Chem. Rev.* **1997**, *97*, 3313−3361.

(7) Späth, A.; Konig, B. Molecular Recognition of Organic Ammonium Ions in Solution Using Synthetic Receptors. *Beilstein J. Org. Chem.* **2010**, Chapter 6.

(8) Gerencsér, J.; Báthori, N.; Czugler, M.; Huszthy, P.; Nógrádi, M. Synthesis of New Optically Active Pyridino- and Pyridono-18-Crown-6 Type Ligands Containing Four Lipophilic Chains. *Tetrahedron: Asymmetry* **2003**, *14*, 2803−2811.

(9) Kim, J. K.; Kim, J.; Song, S.; Jung, O. S.; Suh, H. Enantiomeric Recognition of D- and L-Amino Acid Methyl Ester Hydrochlorides by New Chiral Bis-Pyridino-18-Crown-6 Substituted with Urea, and Diphenyl Groups. *J. Inclusion Phenom. Macrocyclic Chem.* **2007**, *58*, 187−192.

(10) Pirkle, W. H.; Pochapsky, T. C. Considerations of Chiral Recognition Relevant to the Liquid Chromatography Separation of Enantiomers. *Chem. Rev.* **1989**, *89*, 347−362.

(11) Izatt, R. M.; Zhu, C. Y.; Huszthy, P.; Bradshaw, J. S. In *Crown Compounds: Toward Future Applications*; Cooper, S. R., Ed.; VCH, New York, 1992, Chapter 12.

(12) Bailey, P. D.; Everitt, S. R. L.; Morgan, K. M.; Brewster, A. G. The Asymmetric Synthesis and Conformational Analysis of New C2-Symmetric Macrocycles Derived from Head-To-Head Linked α-Amino Acids and Benzene or Pyridine. *Tetrahedron* **2001**, *57*, 1379−1386.

(13) Cunliffe, D.; Kirby, A.; Alexander, C. Molecularly Imprinted Drug Delivery Systems. *Adv. Drug Delivery Rev.* **2005**, *57*, 1836−1853.

(14) Shamaeli, E.; Alizadeh, N. Kinetic Studies of Electrochemically Controlled Release of Salicylate from Nanostructure Conducting Molecularly Imprinted Polymer. *Electrochim. Acta* **2013**, *114*, 409−415.

(15) Kytariolos, J.; Dokoumetzidis, A.; Macheras, P. Power Law IVIVC: An Application of Fractional Kinetics for Drug Release and Absorption. *Eur. J. Pharm. Sci.* **2010**, *41*, 299−304.

(16) Horváth, G.; Huszthy, P. Chromatographic Enantioseparation of Racemic 1-(1-Naphthyl)ethylammonium Perchlorate by a Merrifield Resin-Bound Enantiomerically Pure Chiral Dimethylpyridino-18-Crown-6 Ligand. *Tetrahedron: Asymmetry* **1999**, *10*, 4573−4583.

(17) Bradshaw, J. S.; Huszthy, P.; Wang, T. M.; Zhu, C. Y.; Nazarenko, A. Y.; Izatt, R. M. Enantiomeric Recognition and Separation of Chiral Organic Ammonium Salts by Chiral Pyridino-18-Crown-6 Ligands. *Supramol. Chem.* **1993**, *1*, 267−275.

(18) Bradshaw, J. S.; Nakatsuji, Y.; Huszthy, P.; Wilson, B. E.; Dalley, N. K.; Izatt, R. M. Proton-Ionizable Crown Compounds. 3. Synthesis and Structural Studies of Macrocyclic Polyether Ligands Containing a 4-Pyridone Subcyclic Unit. *J. Heterocycl. Chem.* **1986**, *23*, 353−360.

(19) Bradshaw, J. S.; Huszthy, P.; Koyama, H.; Wood, S. G.; Strobel, S. A.; Davidson, R. B.; Izatt, R. M.; Dalley, N. K.; Lamb, J. D.; Christensen, J. J. Proton-Ionizable Crown Compounds. 8. Synthesis and Structural Studies of Macrocyclic Polyether Ligands Containing a 4-Thiopyridone Subcyclic Unit. *J. Heterocycl. Chem.* **1986**, *23*, 1837−1843.

(20) Izatt, R. M.; Wang, T. M.; Hathaway, J. K.; Zhang, X. X.; Curtis, J. C.; Bradshaw, J. S.; Zhu, C. Y.; Huszthy, P. Factors Influencing Enantiomeric Recognition of Primary Alkyl-Ammonium Salts by Pyridino-18-Crown-6 Type Ligands. *J. Inclusion Phenom. Mol. Recognit. Chem.* **1994**, *17*, 157−175.

(21) Tóth, B.; Pap, T.; Horváth, V.; Horvai, G. Nonlinear Adsorption Isotherm as a Tool for Understanding and Characterizing Molecularly Imprinted Polymers. *J. Chromatogr. A* **2006**, *1119*, 29−33.

(22) Kupai, J.; Lévai, S.; Antal, K.; Balogh, G. T.; Tóth, T.; Huszthy, P. Preparation of Pyridino-Crown Ether−Based New Chiral Stationary Phases and Preliminary Studies on Their Enantiomer Separating Ability for Chiral Protonated Primary Aralkylamines. *Tetrahedron: Asymmetry* **2012**, *23*, 415−427.

(23) Johnson, M. R.; Jones, N. F.; Sutherland, I. O.; Newton, R. F. Formation of Complexes between Aza Derivatives of Crown Ethers and Primary Alkylammonium Salts. Part 8. 12-Crown-4, 15-Crown-5, 21-Crown-7, and 24-Crown-8 Derivatives. *J. Chem. Soc., Perkin Trans. 1* **1985**, 1637−1643.

(24) Beltran, A.; Borrull, F.; Cormack, P. A. G.; Marce, R. M. Molecularly Imprinted Polymer with High-Fidelity Binding Sites for the Selective Extraction of Barbiturates from Human Urine. *J. Chromatogr. A* **2011**, *1218*, 4612−4618.

(25) Chen, Y.; He, X. W.; Mao, J.; Li, W. Y.; Zhang, Y. K. Preparation and Application of Hollow Molecularly Imprinted Polymers with a Super-High Selectivity to the Template Protein. *J. Sep. Sci.* **2013**, *36*, 3449−3456.

(26) Luo, X. B.; Liu, L. L.; Deng, F.; Luo, S. L. Novel Ion-Imprinted Polymer Using Crown Ether as a Functional Monomer for Selective Removal of Pb(II) Ions in Real Environmental Water Samples. *J. Mater. Chem. A* **2013**, *1*, 8280−8286.

(27) Suedee, R. Novel Strategic Innovations for Designing Drug Delivery System Using Molecularly Imprinted Micro/Nanobeads. *Int. J. Pharm. Sci. Rev. Res.* **2013**, *20*, 235−268.

(28) Szekely, G.; Fritz, E.; Bandarra, J.; Heggie, W.; Sellergren, B. Removal of Potentially Genotoxic Acetamide and Arylsulfonate Impurities from Crude Drugs by Molecular Imprinting. *J. Chromatogr. A* **2012**, *1240*, 52−58.

(29) Jabbari, E. In *Biologically-Responsive Hybrid Biomaterials: A Reference for Material Scientists and Bioengineers*; Jabbari, E., Khademhosseini, A., Eds.; World Scientific Publishing Co. Pte. Ltd.: Singapore, 2010.

(30) Costa, P.; Lobo, J. M. S. Modelling and Comparison of Dissolution Profiles. *Eur. J. Pharm. Sci.* **2001**, *13*, 123−133.

(31) Mayes, A. G.; Mosbach, K. Molecularly Imprinted Polymer Beads: Suspension Polymerization Using a Liquid Perfluorocarbon as the Dispersing Phase. *Anal. Chem.* **1996**, *68*, 3769−3774.

DOI: 10.1021/acsami.5b00755
ACS Appl. Mater. Interfaces 2015, 7, 9516−9525